Automated diagnosis of piston slap faults in internal combustion engines: based on a simulation model

Jian Chen (1), Robert Randall (1), Bart Peeters (2) and Herman Van der Auweraer (2)

(1) School of Mechanical and Manufacturing Engineering, University of New South Wales, Sydney 2052 Australia
(2) LMS International, Interleuvenlaan 68, B-3001 Leuven, Belgium

ABSTRACT

The lateral motion of the piston is an inherent kinematic characteristic of reciprocating Internal Combustion (IC) engines. Piston slap is a common mechanical fault in the engine operation. Oversized clearance from scuffing or wear leads to excessive impacts between the piston and cylinder inner wall. Up to now, many researches have investigated the dynamic process of piston slap and some of them have proposed using vibration signals measured on the surface of the block to detect and identify the piston slap faults. However, during the implementation process, all the methods require an expert to interpret the analysis results from measured vibration signals. An Artificial Neural Network (ANN)-based automated system for piston slap diagnosis is described in this paper. The automated diagnostic system consists of three main stages: fault detection, fault localization and severity identification. Simulation models were built to simulate different piston slap faults. Instead of having to experience large numbers of piston slap faults in experiments, simulated data with added random variations (based on a small number of experiments) provided sufficient input data to train the networks. Recent advances by the authors in simulating piston slap are also described in this paper. The effects of the lubrication oil and piston ring were modelled as fixed (free) length spring/damper units, smaller than the clearance. In order to validate and update the simulation model, a small number of experiments with normal clearance and two different oversized piston/inner wall clearances were carried out. Signal processing techniques were applied to extract diagnostic features from the vibration signals. Finally, the experimental cases were used to test the performance of the networks and the results have demonstrated that the developed system can efficiently diagnose different piston slap conditions, including location and severity.

INTRODUCTION

From the perspective of mechanics, many researchers have already investigated the principle of the motion and the impact between the piston and cylinder wall. The impact may happen whenever the side thrust force acting on the piston changes direction. Ungar & Ross (1965) studied the dynamics of lateral piston motions across the cylinder clearance spaces and developed the relationship between the side thrust force and the inertia force and combustion force. They found that the times of occurrence of piston slap in one cycle are dependent on the operating conditions. Haddad & Fortescue (1977) appear to be the earliest researchers to use a computer to simulate the motion of piston/inner wall on the basis of a simplified mathematical model. In the simplified model, the piston and inner wall were modelled as mass points and are connected by spring and damper elements. More recently, Cho et al. (2002) further studied the modelling of piston slap. Similar to Haddad & Fortescue's method, they simplified the piston and inner wall as lumped masses, spring and damper elements, and the parameters were estimated from point mobility experiments. After the impact forces were calculated, they predicted the engine block surface vibration response by convolving the impact forces with measured impulse responses between the cylinder inner walls and engine block outer surfaces. Both Ohta et al. (1987) and Siavoshani (2006) developed 3D models and used Finite Element Method (FEM) to analyse the impact force of piston slap. It should be noted that the flexible contact needs much more computing resource than rigid contact in FEM.

In general, the aims of these studies were focussed on the piston design, including the geometrical and lubrication aspects. On the other hand, oversized piston/inner wall clearance caused by wear during operation is a common mechanical fault of IC engines. Only a limited number of researchers have investigated the technology of using the measured vibration signals to diagnose piston slap faults (Geng & Chen 2007; Li et al. 2010). Moreover, when these vibration-based techniques are applied in a real situation, the piston slap faults cannot automatically be diagnosed from the analysed vibration signals. Artificial Neural Network (ANN)-based automated systems have been successfully applied in the fault diagnostics of rotating machines and they can be an effective tool for the fault diagnostics of reciprocating engines as well. This paper proposes an ANN-based automated system for piston slap diagnosis. The critical issue for the application of ANN to engine diagnostics is having sufficient input data to train the networks and it is uneconomical to achieve this by performing large numbers of experiments with piston slap faults. The latest simulation technology provides a useful service in that the effect of clearance changes may readily be explored without recourse to cutting metal, creating enough training data for the ANN. A series of experiments with two different oversize piston/inner clearance conditions were carried out on a test rig and they provide the evidence needed to validate the simulation model. Accurate simulations of piston impact and the resulting vibration signals may need lots of parameter and function detail, involving kinematic and hydrodynamic issues and the measured vibration in reality is complicated. However, the inputs to the ANN system are the patterns/features of the processed signals rather than all the detailed information of the raw signals. Therefore, the essential requirement for the simulation is to make the features of the processed simulation signals match with real processed signals. In this paper, based on the existing simplified models of piston slap, advanced simulation software (LMS Virtual.Lab) was used to simulate piston slap faults. In particular the former work (Chen et al. 2012) was expanded and the effects of piston ring and lubricant were modelled as fixed (free) length spring/damper units, smaller than the clearance. Finally, the results have demonstrated that the simulation model can create efficient inputs for training purposes and the ANN system can correctly diagnose different piston slap conditions, including location and severity.

EXPERIMENT AND FEATURE EXTRACTION

A Toyota 3S-FE gasoline engine (four-stroke four-cylinder with firing sequence 1-3-4-2) was set up on a test rig. The vibration signals in normal, misfire and piston slap fault conditions were recorded. The purpose of introducing misfires into the different experiments is to verify the robustness of the piston slap diagnostic system. By adjusting the connected dynamometer, the engine was controlled to operate at three constant speed conditions: 1500 rpm, 2000 rpm and 3000 rpm. For each speed, there are three different load conditions: 50 Nm, 80 Nm, and 110 Nm. The normal piston clearance is 0.05mm. After the test with normal and misfire conditions, the cylinder 1 was separately bored with two oversized clearances (3 times and 6 times normal piston clearance) to simulate piston slap faults. The two oversized clearances were advised by the engineers in the engine reconditioning workshop: 3 times normal clearance can represent moderate piston slap and 6 times normal clearance can represent severe piston slap. Even though the cylinder wall was bored around the whole circumference, the impact force is dominated entirely by the clearances in the plane of motion and the mass of the piston. The clearances in the crankshaft axial direction and the detailed shape of piston & cylinder wall have no influence on the impact force. In the later simulation, the motion was also constrained to be in the traverse plane through the centre point of the crank pin. The location of the main response accelerometer is shown in Figure 1. The accelerometer is close to the major thrust side of cylinder 1. The accelerometers were screwed onto studs which were cemented in place with isocyanate cement, with repeatable linear frequency response to more than 10 kHz. The once-per-rev signal was picked up by a proximity transducer, and corresponds to the top dead centre of cylinder 1. The cylinder pressure was measured by a spark plug with integrated cylinder pressure sensor. During the signal processing, the pressure signals were used to separate the firing top dead centre of cylinder 1 from the measured tacho signals. Meanwhile, combustion leakage may happen with the oversized piston/inner clearances; therefore the pressures were measured in different cylinders to check the pressure uniformity. The synchronously averaged pressure was also used to update the combustion chamber pressure of the simulation models in the following section.

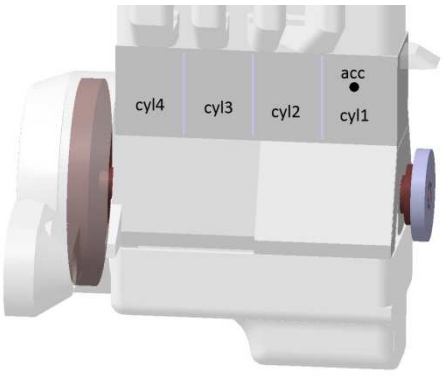

Figure 1. Accelerometer layout and experiment set up

An example of the raw signals is shown in the top part of Figure 2 (2000 rpm/110 Nm). It can be seen that the most obvious piston slap happens just after top dead centre of the firing stroke (the tacho corresponds to the firing top dead centre cylinder 1). Due to the short transient nature of each impact, the measured vibration signals from the piston slap can be considered as a near-periodic series of high frequency bursts and they are also influenced by the high frequency resonances of the structure (engine block) The diagnostic information of interest lies in the repetition frequency and pattern of the bursts rather than their frequency content. Therefore envelope analysis is an appropriate signal processing approach for the detection of the mechanical faults. Moreover, the envelope signals should be deterministic (actually first order cyclostationary) and therefore can be synchronously averaged. The envelope signal was also squared to represent it in power units.

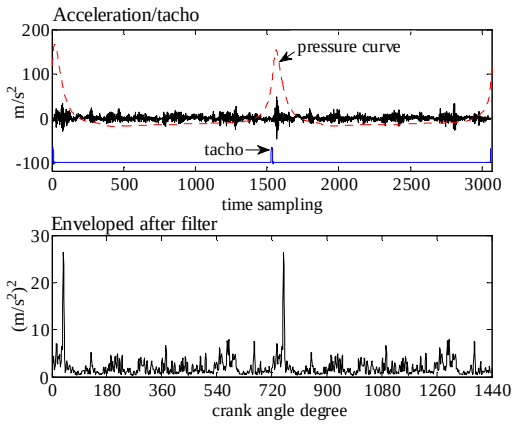

(a) normal condition

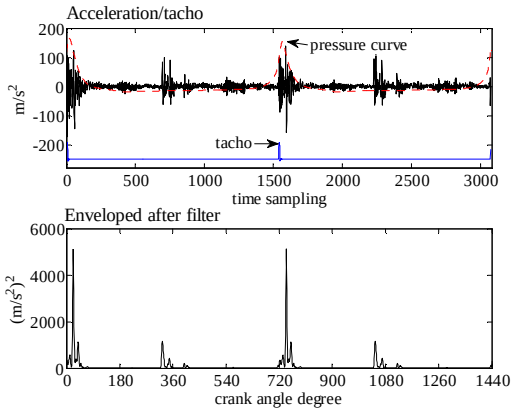

(b) piston slap fault-stage 2

Figure 2. Raw acceleration signal and squared envelopes after filtering

The raw piston slap signals may also contain some low frequency combustion noise and other random mechanical noise. In order to find how the impulsiveness of the measured mechanical fault signals varies with frequency, the "kurtogram" (Antoni & Randall 2006) was applied as a prelude to the envelope processing. In the "kurtogram", the spectral kurtosis is calculated by taking the fourth power of the time/frequency envelope of the signal at each frequency, and averaging its value along the record, then normalising it by the square of the mean square value (Antoni & Randall 2006):

$$K(f) = \frac{H^4(t,f)}{\left[H^2(t,f)\right]^2} - 2 \quad (1)$$

In the equation, the denominator is independent of the window length chosen, but the numerator is affected by it. The "kurtogram" can find the best window for a maximum value of kurtosis which indicates the highest level of impulsiveness of the measured signals.

Two examples of the results from the "kurtogram" are shown in Figure 3, and the brown area indicates the most impulsive frequency range. It was found that the most impulsive fre-

quency ranges in different speeds/loads vary a little. In order to compare piston slap faults for different speeds/loads, the frequency band selections were adjusted and a common frequency band was found. The most important premise of the adjustment is that there is no significant feature change or loss in the succeeding analysis of the envelope. Investigating the polar diagrams after frequency band adjustment for the faults at different speed and load, a common frequency (400-3200Hz) was selected for the piston slap detection. The frequency band selection is also suitable for the future simulation work, because it has been demonstrated that the operational modes of the engine are easy to identify below 4000Hz in the experiments. Based on the "kurtogram" results (400-3200Hz), the squared envelope of the signal after filtering was calculated (examples of enveloped signals are shown in the lower parts of Figure 2).

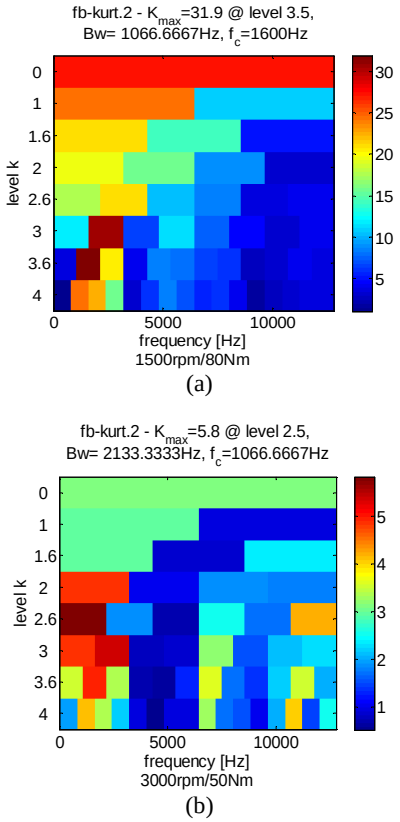

Figure 3. Results from "kurtogram" of piston slap

For the same oversized piston clearance, it was found that the measured signals have a strong relationship with speed/load conditions, i.e. higher speeds and bigger loads have stronger vibration signals. In order to compensate for these relationships in the diagnostic process, the squared enveloped signals were normalized by the ratios from speed/load. After studying the peak values of the enveloped signals at different speeds/loads, an approximate linear relationship was derived and the normalized enveloped signal was taken as:

$$Nor\_enveloped = \frac{Enveloped}{(speed/20)\times(load/100)} \tag{2}$$

Similar to the work of (Desbazeille et al. 2011), for misfire faults, the polar diagram of Fourier coefficients (amplitude and phase, instead of real and imaginary part) of the signals was studied for the feature extraction, although the averaged envelope was used rather than the raw signal. Due to the transient characteristics, the amplitude and phase of the first 40 harmonics of the envelope signal were considered. The amplitude features were used to detect the different faults and identify the severity, and the phase features were used to classify which cylinder had the fault. However, all the candidate features have different sensitivities to the different conditions of the engine. Only some of them may be useful for the pattern recognition of mechanical faults. Therefore, a genetic Algorithm (GA) feature selection method (Ludwig, 2010) was used to assist in the selection of the best features in this situation. Moreover, size-reduced feature inputs can save lots of computing time in the succeeding application of ANNs. The fitness function of the GA selection algorithm was based on Max-Relevance and Min-Redundancy (Ding, 2003). The maximum relevance condition is maximal *H(Y/xi)*:

$$H(Y/x_i) = \frac{1}{|N|}\sum_{x_i\in N} I(Y,x_i) \tag{3}$$

And the minimum redundancy condition is minimal $H(x_i/x_j)$:

$$H(x_i/x_j) = \frac{1}{|N|^2}\sum_{x_i,x_j\in N} I(x_i,x_j) \tag{4}$$

Where N is the selected or desired feature subset, $|N|$ means the number of feature subsets, I is the mutual information of two variables m and n:

$$I(m,n) = \sum_{i,j} p(m_i,n_j)\log\frac{p(m_i,n_i)}{p(m_i)p(n_j)} \tag{5}$$

where $p(m,n)$ is the joint probabilistic distribution of m and n. $p(m)$ and $p(n)$ are marginal probabilities respectively. In the cases of piston slap, the Y is the detection target and the x are the amplitude features.

For the selection of phase features, it was found that most information is contained in the lower harmonics. To find the optimal phase features is not as difficult as the selection of optimal amplitude features. A simple scattering ratio was introduced for the calculation of the phase distribution. Detail of the feature selection on the amplitudes and phases can be obtained from the previous work (Chen et al. 2011).

PRINCIPLE OF PISTON SLAP MODELLING

Piston slap is an impact between the piston and cylinder wall in a reciprocating engine or compressor. It arises when the resultant transverse force exerted by the connecting rod changes direction, causing the piston to leave the side of the cylinder it was previously held against and impact the opposite side (shown in Fig.4).

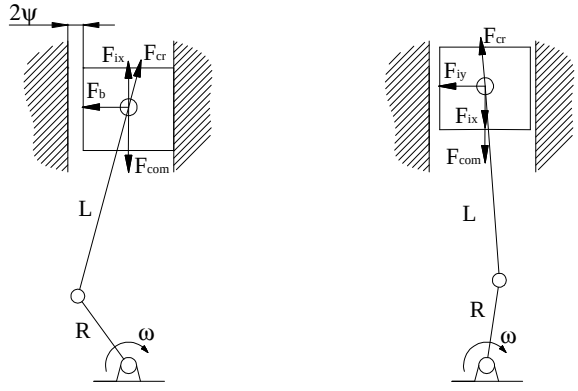

Figure 4. Principle of piston slap

Here, F_{com} is combustion force, F_{cr} is the reaction force of the connecting rod, F_b is the reaction force of the cylinder wall, F_{ix} is the axial inertia force of the piston and F_{iy} is the lateral inertial force of the piston, ψ is the radial clearance, ω is almost constant angular speed of the crankshaft, L is the length of the connecting rod and R is the crank radius. Essentially, the piston slap is due to the periodic change of the transverse component of the reaction force (side-thrust force F_y) by the connecting rod:

$$F_y = \frac{(F_{gas} - F_{ix})\lambda \sin\theta}{\sqrt{1+(\lambda \sin\theta)^2}} = \frac{[F_{gas} - m_1 R\omega_2(\cos\theta + \lambda\cos 2\theta]\lambda \sin\theta}{\sqrt{1+(\lambda \sin\theta)^2}} \quad (6)$$

where m_1 is the mass of the piston, λ is the ratio of L and R. Whenever F_y passes through zero and changes direction it may cause an occurrence of piston slap at some position along the cylinder wall. Similar to the models from (Cho et al. 2002) and (Haddad & Fortescue 1987), the piston and inner wall can be modelled as lumped masses. The effect of the piston ring and lubrication oil was modelled as a viscous damper and spring between the piston and inner wall (shown in Figure 5). The spring and damper are fixed length independent of the clearance, so that they only come into play when the piston is close to the inner wall. The values of the damping and stiffness were obtained from (Haddad & Fortescue 1987), and during the simulation, they were also tuned using the measured vibration signal.

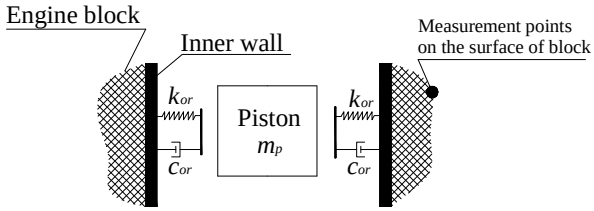

Figure 5. Dynamic model of piston/ inner wall

Even though the translation and rotation of the piston are complicated during the engine operation, in general, there are three contact modes for the piston and inner wall: two point contact, line contact and one point contact. As shown in Figure 6, the line contact mode (the middle one in Figure 6) can be simplified as upper and lower points on one side of piston simultaneously in contact with the inner wall (although the Hertzian stiffness exponent would be slightly different). Therefore, all the contact modes can be considered as point to point contact and the classical Hertz contact theory can be used in the modelling of piston slap.

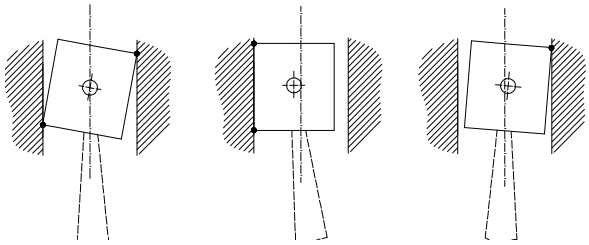

Figure 6. Contact modes of piston/inner wall

The contact force can be calculated from:

$$F_{cont} = k_{cont}\delta^{3/2} \quad (7)$$

Where k_{cont} is the contact stiffness, δ is total deformation of both contact surfaces. The contact stiffness k_{cont} depends on the material properties of the impacting structures and the contact surface geometry.

$$k_{cont} = k\left(1-\left(\frac{1-e^2}{1+e^2}\right)\right)\tanh\left(\frac{2.5V_{pen}}{V_{eps}}\right) \quad (8)$$

Where e is the coefficient of restitution, V_{pen} is penetration velocity, V_{eps} is minimum penetration velocity and the stiffness parameter k can be obtained from (LMS Virtual.Lab manual 2012).

The combustion force acting on the top of the piston can be calculated by Wiebe's functions. The detail of pressure calculation can be obtained from the previous work (Chen et al. 2011)

SIMULATION OF PISTON SLAP FAULTS

The cylinder chamber pressures for different speeds/loads were first calculated in Matlab. The pressure calculation was evaluated and updated using the averaged measured cylinder pressure. The simulation model of piston slaps was built in the Motion module of LMS Virtual.Lab. The calculated cylinder pressures were the inputs to the combustion element in the model. With a tacho element at the crankshaft/block joint and the shift of combustion phase, the firing sequence was set to 1-3-4-2. Based on the proposed model in Figure 5, the piston and inner wall were modelled as rigid to avoid cumbersome flexible contact. Damper and spring elements were used to represent the effect of lubricating oil and piston ring. In order to model the spring/damper units as fixed (free) length, i.e independent of the clearance, a mathematic cubic step function was used (shown in Figure 7). The cubic step function is a blending function. For values of u is less than x_{min}, step has the value y_{min}. For the values of u is greater than x_{max}, step has the value y_{max}. For values of u in between x_{min} and x_{max}, step returns the value of the cubic function fitted between the two points y_{min} and y_{max}. In the piston slap simulation model, the variable u is the distance between piston and inner wall and the outputs of the step functions are stiffness coefficient and damping coefficient. The y_{min} was set to zero. Compared to the Boolean function, the advantage of the cubic step function is that it is free from the problem of parameter instantaneous change, which may cause oscillation in the simulated forces and accelerations.

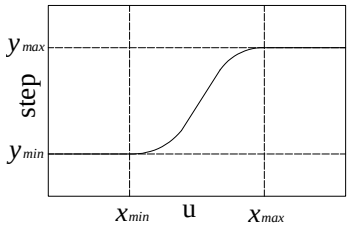

Figure 7. Cubic step function

As shown in Figure 6, the upper and bottom points (4 points for each piston) were defined as spherical contact points. By changing the inner diameter of the inner wall, different piston clearances were created. The main motion components in the simulation models are shown in Figure 8. The mass and inertia properties of most components were measured in experiments, including the crankshaft, connecting rod, engine block and engine head. The inertia properties of some components, such as the piston, were calculated from the geometry in

CATIA, and the geometry was adjusted beforehand to get accurate mass. As shown in Figure 8, the engine block was meshed and its flexible model was updated by the results of experimental modal analysis using LMS Test.Lab. Therefore the accelerations of the surface points of the engine block could be simulated in the model and then correspond to the measured accelerations in the experiments. A brake torque was applied to the output of the crankshaft to simulate the role of the dynamometer.

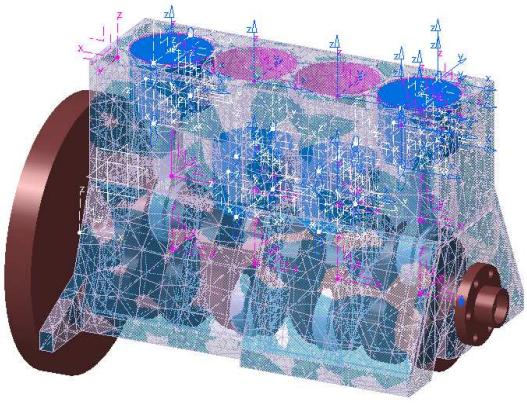

Figure 8. Main motion components

The normal, misfire and piston slap faults in different cylinders were simulated. Based on the analysed results (envelope signals) from the experimental data, some parameters in the simulation were updated and adjusted. All simulated acceleration signals were taken from the surface point where the accelerometer is located in Figure 1. From the simulation model, the contact force and motion of the piston can be obtained. The same data processing tools (enveloping after band pass filtering) were carried out on the simulated accelerations. For the piston slap diagnostic system, the simulations only need to produce the correct envelope signals, so the resonance frequencies do not have to be reproduced exactly. The simulated signal for a certain speed/load condition is deterministic, but in reality the measurement signals have small deviations in different test scenarios, so a variation in the simulated signals should be instituted to create representative cases for the ANN training. The standard deviation of the variations was set by analysing the normal conditions from experiments and was applied to the simulated enveloped signals. The simulated envelope signals of piston slap faults in cylinder 1 are shown in Figure 9.

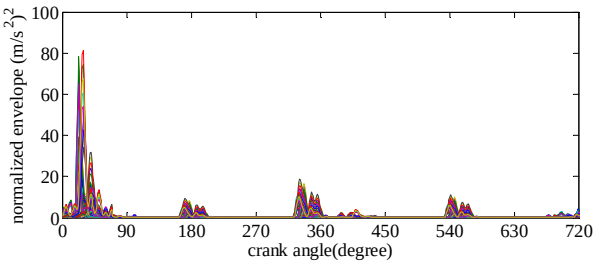

Figure 9. Simulated enveloped signals

ANNS AND EVALUATION RESULTS

Much research has shown that ANNs are a very efficient method to differentiate various faults of rotating machines (Randall 2001; Paya et al. 1997; Alguindigue et al. 1993). ANNs can make judgments about inputs they have never been presented with before, based on what they were delivered in the past. For details of ANNs refer to (Hagan et al. 1996). Even through only a limited number of experiments were carried out on the test rig, the simulation results from the developed models provide adequate data for the training of ANNs. For the diagnostics of piston slap faults, three network systems were designed (shown in Figure 10). The first stage is the piston slap detection stage and the inputs to the networks are the selected amplitude features of the enveloped signals. In the second stage, the neural network localizes which cylinder has piston slap faults and the inputs to the network are the selected phase features of the envelope signals. In the third stage, based on the detection and location results, the severity of the piston slap faults is identified. The detection stage and severity identification stage were enacted by multi-layer perceptron (MLP) networks and the localization stage was enacted by probabilistic neural networks (PNN).

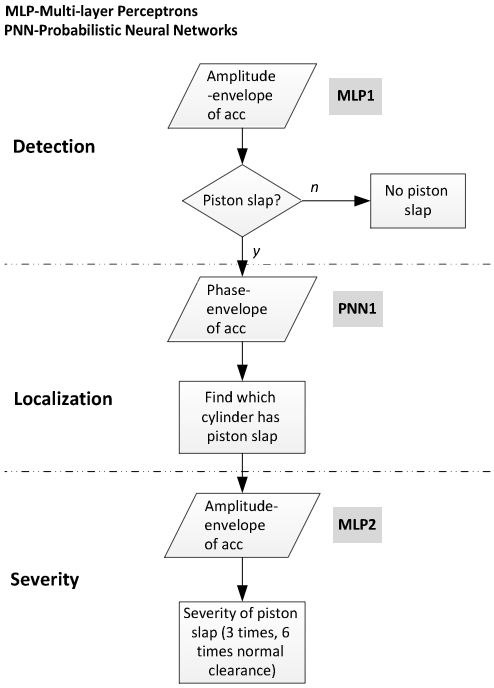

Figure 10. Structure of the ANNs

All training data are the extracted features from the simulated enveloped signals. The training cases included 288 piston slap faults and 112 cases with normal piston clearance (but some of them having combustion faults). 49 experimental cases were used to test the network. For the MLPs in the severity identification stage, the training and evaluation group are reduced to piston slap cases for the individual cylinder only. The output of the MLP in the detection stage is from 0 to 1; 0 for normal condition, and 1 for fault condition. In the severity identification stage, the output 0.5 means 3 times oversized piston slap faults and 1 means 6 times oversized piston slap faults. A fitness criterion was introduced to test the performance of detection stage MLPs:

$$Error = \sum_{i=1}^{N} \left| (ANN(i) - VAL(i) \right| \quad (10)$$

where ANN is the output of the MLPs and VAL is the corresponding target number (N = 49). The configuration of MLP is shown in Figure 11.

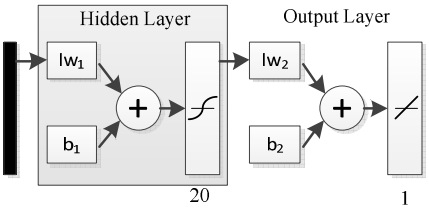

Figure 11. The diagram of the MLP networks

Due to their advantage for classification problems, PNNs were used to identify which cylinder has piston slap faults. A PNN network is based on the weighted-neighbour method and was proposed by Specht (1990). The outputs of the PNN for the mechanical fault diagnostics are the integer numbers 1, 2, 3 and 4, which directly indicate the cylinder number.

The outputs of MLP1 are shown in Figure 12. In reality, there are piston slap faults for case 1 to 18 and 33 to 42. The final fitness criterion is 0.2253, so the MLP1 100% correctly detected all piston slap faults.

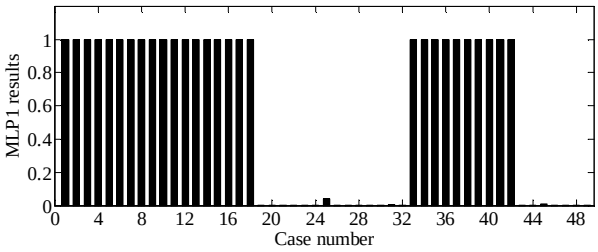

Figure 12. Output of MLP1

For the localization of the piston slap faults, using the selected phase features as inputs, the PNN also achieved a good classification result. The results 100% match with the real situation of the evaluation cases: all piston slap faults (28 cases) happen in cylinder 1 in the experiments.

After the piston slap detection stage, the severity identification became more specific. The output results of MLP2 are shown in Figure 13. It can be seen that MLP2 100% correctly identified the severity identification of the piston slap faults. It is also found that, in spite of the normalization beforehand, the severity identification is more sensitive to the speed and load conditions. The network needs more computing time (more epochs) to achieve the training goal and the final fitness criterion (1.8455) is larger compared to the detection stage.

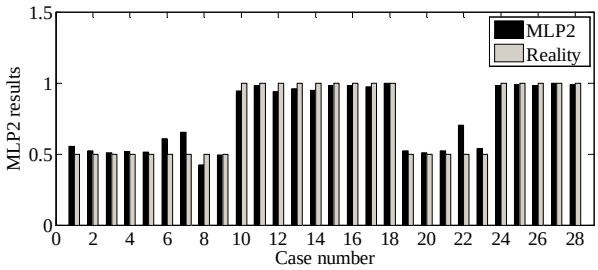

Figure 13. Output of MLP2

CONCLUSION

This paper expands the former works and updates the modelling of piston slap faults, with fixed length spring and damper units. In the simulation model, a cubic step function was used to control the effect of fixed length spring and damper units. The developed simulation model was used to simulate piston slap faults in different cylinders for different speed/load conditions. Beforehand, a small number of experiments were carried out so as to evaluate and update the simulation models. Signal envelope processing with band pass filtering was used to process experimental signals to extract potential features. In the simulation model, the point to point contact mode was applied for modelling the contact of piston and inner wall. The standard deviations derived from experimental measurements in normal condition were applied to the simulated enveloped signals to create suitably varied cases. The simulated acceleration signals were processed by the same signal processing techniques as the measurements and the selected features from the processed data were used to train the networks. The processed simulated data provided enough data for the training of the ANNs. Finally, it has been demonstrated that even though the networks were only trained by simulation data, they can efficiently detect the piston slap faults in real tests and identify the location and severity of the faults.

ACKNOWLEDGEMENTS

The author would like to convey special gratitude to the Australian Research Council and LMS International for sponsoring this research under Linkage Project LP0883486. Part of the research was conducted in the frame of the ITEA 2 project 11004 MODRIO (Model driven physical systems operation). The financial support of the IWT (Flemish Agency for Innovation by Science and Technology) is gratefully acknowledged.

REFERENCES

Alguindigue I. E., Buczak A. L. & Uhrig R. E., 1993, 'Monitoring and Diagnosis of Rolling Element Bearings Using Artificial Neural Networks', *IEEE Transaction on Industrial Electronics*, vol. 40, no. 2, pp.209-217

Antoni J., Randall R. B., 2006, 'The spectral kurtosis: application to the vibratory surveillance and diagnostics of rotating machines', *Mechanical Systems and Signal Processing*, vol. 20, pp. 308–331

Chen J, Randall R. B., Peeters B., Van der Auweraer H & Desmet W., 2012, 'Automated diagnosis of piston slap in engines', *CM2012 & MFPT2012*, London, UK

Chen, J., Randall, R.B., Peeters, B., Desmet, W. & Van der Auweraer, H., 2011 'Artificial neural network based fault diagnosis of IC engines', *Workshop on Mid-frequency Analysis of Noise and Vibration, (To be published in Key Engineering Materials)*, Krakow, Poland

Cho S.H., Ahn S.T. & Kim Y.H., 2002, 'A simple model to estimate the impact force induced by piston slap', Journal of Sound and Vibration, vol. 255, no. 2, pp.229-242

Desbazeille M., Randall R.B., Guillet F., El Badaoui, M. & Hoisnard, C., 2011, 'Model-based diagnosis of large diesel engines based on angular speed variations of the crankshaft', *Mechanical System and Signal Processing*, vol 24, no 5, pp. 1529-1541

Ding C., Peng H., 2003, 'Minimum Redundancy Feature Selection from Microarray Gene Expression Data'. *Proceedings of the Computational Systems Bioinformatics*, Stanford, USA, pp.523-529

Geng Z., Chen J., 2007, 'Investigation into piston-slap-induced vibration for engine condition simulation and monitoring', *Journal of Sound and Vibration*, vol. 282, no. 3-5, pp.735–751

Haddad S. D. & Fortescue P. W., 1987, 'Simulating Piston Slap by an Analog Computer', *Journal of Sound & Vibration*, vol. 72, no. 1, pp 79-93

Hagan M. T., Demuth H. B. & Beale M. H., 1996, 'Neural Network Design', PWS Publishing, Boston, USA

Li Y.J. , TSE P.W. &Yang X., 2010, 'EMD-based fault diagnosis for abnormal clearance between contacting components in a diesel engine'. *Mechanical Systems and Signal Processing* , vol. 24, no. 1, pp.193-210

Ludwig O. & Nunes U., 2010, 'Novel Maximum-Margin Training Algorithms for Supervised Neural Networks', *IEEE Transaction on Neural Networks*, vol. 21, no. 6, pp.972-983

LMS Virtual.Lab manual, 2012, Leuven, Belgium

Ohta K., Irie Y., Yamamoto K. & Ishikawa H., 1987, 'Piston slap induced noise and vibration of internal combustion engines', SAE Paper, 870990

Paya B. A., Esat I. L. & Badi M. N. M., 1997, 'Artificial neural network based fault diagnostics of rotating machineryusing wavelet transforms as a preprocessor'. *Mechanical Systems and Signal Processing*, vol. 11, no. 5 pp.751–765

Randall R.B., 2001, 'Training neural networks for bearing diagnostics using simulated feature vectors'. *AI-MECH Symposium*, Gliwice, Poland

Siavoshani J. S., 2006, 'Basic analytical modelling of the piston slap in conjunction with engine block vibration', *International Journal of Vehicle Noise and Vibration*, vol. 2, no. 3, pp. 209 – 226

Specht F. D., 1990, 'Probabilistic Neural Networks and the Polynomial Adaline as Complementary Techniques for Classification', *IEEE Transactions on Neural Networks*, vol. 1, no. 1, pp. 111-121

Ungar E. E. & Ross D., 1965, 'Vibrations and noise due to piston-slap in reciprocating machinery', *Journal of Sound and Vibration*, vol. 2, no. 2, pp. 132-146